1   **Metabolic biomarkers of response to the AKT inhibitor MK-2206 in pre-clinical**

2   **models of human colorectal and prostate carcinoma**

3

4   N M S Al-Saffar[1*], H Troy[1†], A-C Wong Te Fong[1], R Paravati[1], L E Jackson[1], S

5   Gowan[2], J K R Boult[1], S P Robinson[1], S A Eccles[2], T A Yap[3,4‡], M O Leach[1*] and Y-

6   L Chung[1*]

7

8   [1]Cancer Research UK Cancer Imaging Centre, Division of Radiotherapy and Imaging.

9   The Institute of Cancer Research and The Royal Marsden NHS Foundation Trust,

10   London, SW7 3RP, United Kingdom. [2]Cancer Research UK Cancer Therapeutics

11   Unit, Division of Cancer Therapeutics. The Institute of Cancer Research, London,

12   SW7 3RP, United Kingdom. [3]Drug Development Unit, The Royal Marsden NHS

13   Foundation Trust, London, SW7 3RP, United Kingdom. [4]Division of Clinical Studies,

14   The Institute of Cancer Research, London, SW7 3RP, United Kingdom.

15

16   [*]Corresponding Authors:

17   Dr. Nada Al-Saffar

18   Cancer Research UK Cancer Imaging Centre, Division of Radiotherapy and Imaging

19   The Institute of Cancer Research and The Royal Marsden NHS Foundation Trust

20   123 Old Brompton Road, SW7 3RP, London, United Kingdom

21   Tel: +44 (0)20 8722 4686

22   Fax: +44 (0)20 8661 0846

23   Email: nada.al-saffar@icr.ac.uk

24

25

26 Prof. Martin Leach

27 Cancer Research UK Cancer Imaging Centre, Division of Radiotherapy and Imaging

28 The Institute of Cancer Research and The Royal Marsden NHS Foundation Trust

29 123 Old Brompton Road, SW7 3RP, London, United Kingdom

30 Tel: 020 8661 3338

31 Fax: 020 8661 0846

32 Email: Martin.Leach@icr.ac.uk

33

34 Dr. Yuen-Li Chung

35 Cancer Research UK Cancer Imaging Centre, Division of Radiotherapy and Imaging

36 The Institute of Cancer Research and The Royal Marsden NHS Foundation Trust

37 123 Old Brompton Road, SW7 3RP, London, United Kingdom

38 Tel: +44 (0)20 8722 4321

39 Fax: +44 (0)20 8661 0846

40 Email: Yuen-Li.Chung@icr.ac.uk

41

42 [†]Current address: Abbott Ireland Diagnostics Division, Pregnancy and Fertility Team,

43 Lisnamuck, Longford, Ireland.

44

45 [‡]Current address: The University of Texas MD Anderson Cancer Center, Houston,

46 TX, USA

47

48 Running title: Metabolic biomarkers of response to AKT inhibition

49

50 Key words: AKT, MRS, biomarkers, phospholipid metabolism.

51

52 **Abstract**

53 **Background:** AKT is commonly overexpressed in tumours and plays an important

54 role in the metabolic reprogramming of cancer. We have used magnetic resonance

55 spectroscopy (MRS) to assess whether inhibition of AKT signalling would result in

56 metabolic changes that could potentially be used as biomarkers to monitor response to

57 AKT inhibition.

58 **Methods:** Cellular and metabolic effects of the allosteric AKT inhibitor MK-2206

59 were investigated in HT29 colon and PC3 prostate cancer cells and xenografts using

60 flow cytometry, immunoblotting, immunohistology and MRS.

61 **Results:** *In vitro* treatment with MK-2206 inhibited AKT signalling and resulted in

62 time-dependent alterations in glucose, glutamine and phospholipid metabolism. *In*

63 *vivo*, MK-2206 resulted in inhibition of AKT signalling and tumour growth compared

64 with vehicle-treated controls. *In vivo* MRS analysis of HT29 subcutaneous xenografts

65 showed similar metabolic changes to those seen *in vitro* including decreases in the

66 tCho/water ratio, tumour bioenergetic metabolites and changes in glutamine and

67 glutathione metabolism. Similar phosphocholine changes compared to *in vitro* were

68 confirmed in the clinically relevant orthotopic PC3 model.

69 **Conclusion:** This MRS study suggests that choline metabolites detected in response

70 to AKT inhibition are time- and microenvironment-dependent, and may have

71 potential as non-invasive biomarkers for monitoring response to AKT inhibitors in

72 selected cancer types.

73

Background

The AKT/PKB (Protein Kinase B) serine/threonine kinase, with three different isoforms: AKT1, AKT2 and AKT3, is one of the core components of the PI3K signalling cascade, regulating cell proliferation, survival and metabolism, and is frequently activated in cancer (Manning and Toker, 2017). Multiple AKT inhibitors are now at various stages of clinical development (Brown and Banerji, 2017; Khan *et al*, 2013; Nitulescu *et al*, 2016). AKT inhibitors fall predominantly into two classes: ATP-competitive inhibitors and allosteric inhibitors of AKT (Brown and Banerji, 2017; Khan *et al*, 2013; Nitulescu *et al*, 2016). MK-2206 is a potent oral allosteric pan-AKT inhibitor with potential anti-neoplastic activity and is currently being evaluated in numerous clinical trials (Brown and Banerji, 2017; Khan *et al*, 2013; Nitulescu *et al*, 2016). Single-agent trials with this agent have generally shown anti-proliferative, rather than anti-tumour activity, with stable disease identified as the best overall response (Ahn *et al*, 2015; Yap *et al*, 2011; Yap *et al*, 2014). Therefore, identification of non-invasive biomarkers of target inhibition and potentially of tumour response would be of value in the clinical development of the AKT inhibitor MK-2206.

Reprogrammed metabolism is one of the hallmarks of cancer (Hanahan and Weinberg, 2011; Pavlova and Thompson, 2016). As many oncogenic signalling pathways that regulate cancer have also been shown to regulate metabolism (Iurlaro *et al*, 2014; Tarrado-Castellarnau *et al*, 2016), targeting those signalling pathways with drugs such as MK-2206 is expected to impact on metabolic intermediates. Assessment of the metabolic effects of drug treatment using functional imaging modalities, such as magnetic resonance spectroscopy (MRS) and metabolic PET, to provide an early

4

100 treatment response biomarkers to molecularly targeted drugs is being increasingly

101 investigated for clinical biomarker discovery (Beloueche-Babari *et al*, 2010;

102 Beloueche-Babari *et al*, 2011; Moestue *et al*, 2011; Serkova and Eckhardt, 2016;

103 Workman *et al*, 2006).

104

105 MRS provides a non-invasive and non-ionizing method of detecting various

106 tissue metabolites *in vitro*, *ex vivo* and *in vivo* (Gadian, 1995). Numerous studies have

107 investigated MRS-detectable metabolic biomarkers in response to novel targeted

108 therapies that are in pre-clinical development or early phase clinical evaluation

109 including inhibitors of HSP90, MAPK, HDAC, PI3K/AKT/mTOR and related

110 pathways, reviewed in (Beloueche-Babari *et al*, 2010; Beloueche-Babari *et al*, 2011;

111 Moestue *et al*, 2011).

112

113 Using MRS, we and others have previously reported alterations in the levels of

114 choline metabolites and/or lactate in response to different PI3K/mTOR pathway

115 inhibitors *in vitro* and *in vivo* in various cancer models (Al-Saffar *et al*, 2010; Al-

116 Saffar *et al*, 2014; Beloueche-Babari *et al*, 2006; Chaumeil *et al*, 2012; Esmaeili *et al*,

117 2014; Euceda *et al*, 2017; Koul *et al*, 2010; Lee *et al*, 2013; Moestue *et al*, 2013; Phyu

118 *et al*, 2016; Venkatesh *et al*, 2012). However to the best of our knowledge, metabolic

119 biomarkers for AKT inhibitors have only been evaluated *in vitro* and *ex vivo* in breast

120 cancer models (Moestue *et al*, 2013; Phyu *et al*, 2016; Su *et al*, 2012), and there are

121 no previous metabolic biomarker studies *in vivo* in tumour xenografts. In one study

122 (Su *et al*, 2012), treatment of MCF-7 and MDA-MB-231 breast cancer cells with the

123 alkylphospholipid AKT inhibitor perifosine resulted in decreases in PC and lactate

124 production. Two studies reported different results using the allosteric AKT inhibitor

125   MK-2206, which provides greater specificity, reduced side-effects and less toxicity

126   compared to alkylphospholipid AKT inhibitors (Nitulescu *et al*, 2016). A decrease in

127   PC levels was observed *in vitro* in MDA-MB-468 breast cancer cells (Phyu *et al*,

128   2016), while an increase in PC and a decrease in lactate levels were detected *ex vivo*

129   in basal-like breast cancer tumours following treatment with MK-2206 (Moestue *et al*,

130   2013).

131

132   In view of the inconsistent published findings with the allosteric AKT inhibitor

133   MK-2206, and the lack of *in vivo* studies in cancer models, we set out to assess the

134   metabolic changes in response to MK-2206 both *in vitro* and *in vivo* in subcutaneous

135   and orthotopic animal xenograft models of colon and prostate cancer, with potential to

136   develop these metabolic changes as non-invasive biomarkers for monitoring response

137   in clinical trials.

138

139   Our results show that treatment with the AKT inhibitor MK-2206 results in

140   metabolic changes detectable with MRS. Importantly, a decrease in the total choline

141   (tCho)/water ratio was observed in the more clinically relevant orthotopic model of

142   the PC3 prostate cancer and therefore may provide a potential non-invasive biomarker

143   for monitoring response to MK-2206 during clinical trials.

144

Materials and Methods

Cell culture and treatment. The human PTEN null PC3 prostate adenocarcinoma and *PIK3CA* mutant HT29 colorectal carcinoma cell lines (American Type Culture Collection) were cultured in DMEM (Life Technologies) supplemented with 10% fetal calf serum (PAA labs Ltd), 100 U/mL penicillin, and 100 µg/mL streptomycin (Life Technologies) at 37°C in 5% CO_2. Cell viability was routinely >90%, as judged by trypan blue exclusion. All cell lines were shown to be mycoplasma free using a PCR-based assay (Surrey Diagnostics Ltd) and were authenticated in our laboratory by short tandem repeat (STR) profiling.

Both cell lines were treated with the orally active, highly selective non-ATP competitive allosteric AKT inhibitor MK-2206 (Merck & Co., Inc.). GI_{50} values (concentrations causing 50% inhibition of proliferation for tumour cells) were determined using the sulforhodamine B assay following 96 h continuous exposure to compounds (Raynaud *et al*, 2007). At the required time points, cells underwent trypsinization and trypan blue exclusion assay (Al-Saffar *et al*, 2014). The effect of treatment on cell number was monitored by counting the number of viable attached cells in a treated flask and comparing that number with the number of attached cells in a control flask.

Flow cytometry. Cell cycle analysis was performed as previously described (Al-Saffar *et al*, 2014).

Immunoblotting. Western blotting was performed as previously described (Al-Saffar *et al*, 2014). Western blots were probed for pAKT (Ser473; 4060), AKT (9272),

7

170   pRPS6 (Ser240/244; 2215), RPS6 (2217), HK2 (2106), PARP (9542), LDHA (3582),

171   β-Actin (4967), all from Cell Signaling Technology, and CHKA (HPA0241153) from

172   Sigma. Blots were revealed with peroxidase-conjugated secondary anti-rabbit (GE

173   Healthcare NA9340) or anti-mouse (DAKO P0260) antibodies followed by ECL

174   chemiluminescence solution (Amersham Biosciences).

175

176   ***In vitro* ^{1}H- and ^{31}P-MRS of cell extracts.** The same number of cells per flask were

177   seeded at the beginning of the experiment then at the selected time points; cells were

178   pooled from the number of flasks required to achieve an average cell number of 3×10^7

179   cells, which differed depending on the expected effect of treatments on cell number.

180   To obtain an MR spectrum, cells were extracted from cultured cells using the dual

181   phase extraction method, as previously described (Al-Saffar *et al*, 2014; Tyagi *et al*,

182   1996). Briefly, cells were rinsed with ice-cold saline and fixed with 10 mL of ice-cold

183   methanol. Cells were then scraped off the surface of the culture flask and collected

184   into tubes. Ice-cold chloroform (10 mL) was then added to each tube followed by an

185   equal volume of ice-cold deionized water. Following phase separation, the solvent in

186   the upper methanol/water phase was removed by lyophilisation. Prior to acquisition of

187   the MRS spectra, the water-soluble metabolites were resuspended in deuterium oxide

188   (D_2O) for ^{1}H-MRS or D_2O with 10 mM EDTA (pH 8.2) for ^{31}P-MRS. For

189   extracellular metabolite analysis, 500 μL of cell growth medium was mixed with 100

190   μL of D2O containing sodium 3-trimethylsilyl-2,2,3,3-tetradeuteropropionate as an

191   internal reference (TSP; 2.7 mM). ^{1}H-MRS and ^{1}H-decoupled ^{31}P-MRS spectra were

192   acquired at 25°C on a 500 MHz Bruker spectrometer (Bruker Biospin, Coventry, UK)

193   using a 90-degree flip angle, a 1 s relaxation delay, spectral width of 12 ppm, 64 K

194   data points, and HDO resonance suppression by presaturation for ^{1}H-MRS and a 30°

195 flip angle, a 1 s relaxation delay, spectral width of 100 ppm, and 32 K data points for

196 ^{31}P. Metabolite contents were determined by integration and normalised relative to the

197 peak integral of an internal reference [TSP (4.8 mM) for ^{1}H-MRS, and

198 methylenediphosphonic acid (MDPA; 2 mM) for ^{31}P-MRS] and corrected for signal

199 intensity saturation (^{31}P-MRS) and the number of cells extracted per sample.

200

201 *In vivo* **tumour propagation.** All animal experiments were performed in accordance

202 with local and national ethical review panel, the UK Home Office Animals (Scientific

203 Procedures) Act 1986 and the United Kingdom Coordinating Committee on Cancer

204 Research Guidelines for the Welfare of Animals in Experimental Neoplasia

205 (Workman *et al*, 2010).

206

207 **Subcutaneous HT29 and PC3 tumour xenografts.** Male NCr nude mice were

208 injected subcutaneously in the flank with 5×10^{6} HT29 (human colon) or PC3 (human

209 prostate) carcinoma cells. Tumour volume was calculated by measuring the length,

210 width, and depth using calipers and the ellipsoid formula L x W x D x ($\pi/6$). Once the

211 tumours reached ~400 mm^{3}, the animals were divided to two groups. One group was

212 treated with 2 doses of 120 mg/kg of MK-2206 on alternate days (Day 1 and 3) via

213 p.o. and the other group with vehicle alone (10% DMSO in saline).

214

215 **Orthotopic PC3 tumour xenografts.** PC3 cells (5×10^{5}) were inoculated in the

216 ventral prostate gland of nude mice. Once the tumours were palpable, animals were

217 treated with 2 doses of 120 mg/kg of MK-2206 on alternate days (Day 1 and 3) via

218 p.o. or vehicle alone (10% DMSO in saline).

219

220 ***In vivo* MRS of HT29 and PC3 tumours.** Mice were anesthetised with a single

221 intraperitoneal injection of a fentanyl citrate (0.315 mg/mL) plus fluanisone [10

222 mg/mL (Hypnorm; Janssen Pharmaceutical Ltd., High Wycombe, UK)], midazolam

223 [5 mg/mL (Hypnovel; Roche, Welwyn Garden City, UK)], and sterile water (1:1:2) at

224 a dose of 9 mL/kg. They were placed in the bore of a 7 Tesla Bruker MR System

225 spectrometer (Bruker Biospin, Coventry, United Kingdom) with HT29 and PC3

226 tumours positioned in the centre of a 15 mm two-turn ^{1}H/^{31}P surface coil. *In vivo*

227 localised PRESS ^{1}H-MRS of the tumours was carried out at 37°C on Day 0 (before

228 treatment) and the last day of treatment (Day 3). 4 mm x 4 mm x4 mm voxels were

229 selected from fast spin-echo images and shimmed using a localised sequence. The

230 localised PRESS with water suppression was used to detect choline with a repetition

231 time of 4 s, echo times 136 ms and 64 transients. 4 transients were used to acquire the

232 unsuppressed water spectra with the same acquisition parameters as above. Image-

233 selected *in vivo* spectroscopy (ISIS) ^{31}P-MR spectra were also obtained in

234 subcutaneous PC3 tumours with a repetition time of 2 s and 64 transients. After the

235 final MRS scan, tumours were excised and stored at for subsequent *ex vivo* ^{1}H- and

236 ^{31}P-MRS, MSD$^{®}$ assays or immunohistochemical analysis.

237

238 ^{1}H- and ^{31}P-MR spectra were analysed using the JMRUI programme to pre-process,

239 fit and quantify peak areas of the observed metabolites. Choline levels are expressed

240 as a ratio relative to the water (tCho/water) signal following corrections for the

241 number of averages and receiver gains, as these two parameters were different for the

242 acquisitions of water and choline spectra. Phosphomonoesters (PMEs) were expressed

243 as ratios relative to total phosphorus (PMEs/total P) signals.

244

245 **Meso Scale Discovery (MSD®) assay.** Tumour pharmacodynamic biomarkers for

246 MK-2206 were assessed by a MSD® multispot electrochemiluminescence

247 immunoassay system to detect pP70S6K (Thr421/Ser424), total P70S6K, pAKT

248 (Ser473), pAKT (Thr308), total AKT, pRPS6 (Ser235/236), pRPS6 (Ser240/244) and

249 total RPS6 in 10 mg tumour lysate of vehicle and MK-2206 treated tumours

250 according to the manufacturer's instructions (Meso Scale Discovery, Gaithersburg,

251 USA).

252

253 *Ex vivo* **MRS of tumour extracts.** 100- 200 mg of the freeze-clamped tumours were

254 finely grinded in liquid nitrogen and extracted using ice-cold methanol, water and

255 chloroform (1:1:1). The aqueous phase was separated, freeze-dried and reconstituted

256 in 650 µl D_2O. 50 µL of 44 mM TSP in D_2O was added to the samples for ^{1}H

257 chemical shift calibration and quantification. The samples were then placed in 5 mm

258 NMR tubes and sample pH was adjusted to 7 using perchloric acid or potassium

259 hydroxide. ^{1}H-MRS of the tumour extracts was performed on a Bruker 500 MHz

260 nuclear magnetic resonance system (Bruker Biospin, Coventry, United Kingdom) and

261 spectra were acquired using a pulse and collect NMR sequence with presaturation for

262 water suppression; 7500 Hz spectral width, 32 K time domain points, 2.7 s relaxation

263 delay and 256 scans at 298 K. After ^{1}H-MRS, 50 µL of 60 mM EDTA was added to

264 each sample for chelation of metal ions and 25 µL of 10 mM MDPA was added to the

265 samples for ^{31}P chemical shift calibration and quantitation. The pH was again adjusted

266 to 7 and ^{31}P-MRS was performed with 12000 Hz spectral width, 32K time domain

267 points, 5 s relaxation delay and 3000 scans at 298 K (Chung, 2017).

268 MR spectra were analysed using the Bruker Topspin-3.2 software package (Bruker

269 Biospin, Coventry, UK). Spectra were processed by using exponential multiplication

270 with a line broadening of 0.3 Hz and 3 Hz for ^{1}H- and ^{31}P-MR spectra, respectively,

271 then followed by Fourier transform, zero- and first-order phase correction, baseline

272 correction and spectral peak integration integration. Spectral assignments were based

273 on literature values (Chung, 2017; Sitter *et al*, 2002). Water-soluble metabolites

274 measured by ^{1}H and ^{31}P-MRS were quantified relative to TSP or MDPA, respectively,

275 and standardised to tumour weight (Chung, 2017).

276

277 **Immunohistochemistry.** Tumour xenografts were fixed in 10% formaldehyde and

278 routinely processed for paraffin embedding. For histological evaluation, 5 μm-thick

279 paraffin wax sections were cut and stained with haematoxylin and eosin (H&E).

280 Expression of caspase-3 (apoptotic marker), CD31 (micro-vessel density) and Ki67

281 (proliferation marker) were determined by immunohistochemistry, using the

282 streptavidin-biotin peroxidase technique. Briefly, sections of 5 μm were

283 deparaffinised in xylene and rehydrated through graded ethanol concentrations up to

284 distilled water for 30 min. Antigen retrieval was performed by microwaving the

285 sections in 10 mM sodium citrate buffer pH 6 at 10 min intervals for a total of 20 min

286 and cooling for 1 h at room temperature (RT). Endogenous peroxidase activity was

287 blocked by incubating the sections in a solution of 3% hydrogen peroxide for 20 min

288 at RT. After washing in PBS (phosphate buffer saline), sections were incubated with

289 the primary polyclonal rabbit anti-human caspase-3 (1:50, Abcam ab2302),

290 monoclonal rabbit anti-human CD31 (1:50, Millipore 04-1074) mouse monoclonal

291 anti-human Ki67 (1:75, DAKO M7240) antibodies, overnight at 4°C. The sections

292 were washed with PBS and incubated with a biotinylated secondary antibody for 45

293   min, followed by an incubation with streptavidin-biotin horseradish peroxidase

294   complex (DAKO) for another 45 min, at RT. Staining was carried out using a solution

295   3,3'-diaminobenzidine (DAB-Sigma), and lightly counterstained with Harris

296   haematoxylin.

297

298   **Evaluation of staining.** Sections known to express high levels of caspase-3

299   (pancreas), CD31 (liver) and Ki67 (tonsil) were included as positive controls, while

300   negative control slides were incubated with PBS. Caspase-3 and Ki67 immuno-

301   stained slides were assessed by light microscopy and scored with ImageJ (1.50i). A

302   semi-quantitative method was used to score the microvessels stained with CD31

303   (Bosari *et al*, 1992). Three fields showing the highest number of microvessels were

304   selected using light microscopy and the number of micovessels in these fields were

305   then manually counted and averaged. Each section was scored by 2 independent

306   observers at x200 magnification.

307

308   **Statistical analysis.** Data are presented as the mean ± SD (*in vitro*) or mean ± SEM

309   (*in vivo* and *ex vivo*) and n ≥ 3. Statistical significance of differences was determined

310   by Student's standard t-tests with a *P* value of ≤ 0.05 considered to be statistically

311   significant.

312   **Results**

313   *In vitro* **investigation of molecular and metabolic effects of treatment with MK-**

314   **2206 in PC3 human prostate cancer cells.** The PTEN null human prostate cell line

315   PC3 was treated with MK-2206 for 6, 12 and 24 h at a pharmacologically active

316   concentration corresponding to $5xGI_{50}$ ($GI_{50} = 5$ μM). Inhibition of the AKT pathway

317   was evident at all time points as indicated by decreased phosphorylation of AKT

318   (Ser473) and RPS6 (Ser240/244) in treated cells compared to their controls (Figure

319   1A). Treatment with MK-2206 also induced apoptosis which was evident at 12 and 24

320   h following treatment as indicated by PARP cleavage detected by immunoblotting

321   (Fig 1A). Inhibition of cell growth (down to $66 \pm 10\%$, $P = 0.0001$) and a G1 cell

322   cycle arrest was only detectable at 24 h post treatment (Figure 1B).

323

324   ^{31}P-and ^{1}H-MRS of aqueous extracts from PC3 cells treated *in vitro* with the

325   AKT inhibitor MK-2206 ($5xGI_{50}$) was used to identify potential biomarkers of AKT

326   pathway inhibition compared to controls (Figure 1C). Analysis of metabolites

327   detected with ^{31}P-MRS showed a significant decrease ($P \leq 0.02$) in the levels of

328   phosphoethanolamine (PE), phosphocholine (PC) and NTP which was evident at 6 h

329   and was maintained at 24 h (Table 1). Levels of glycerophosphoethanolamine (GPE)

330   and glycerophosphocholine (GPC) were reduced for up to 12 h ($P \leq 0.001$) but then a

331   significant increase ($P \leq 0.01$) was observed at 24 h (Table 1). A significant decrease

332   ($P \leq 0.04$) in the levels of phosphocreatine (PCr) was also detected at 12 h and was

333   maintained at 24 h following treatment with MK-2206. ^{1}H-MRS confirmed changes

334   in PC and GPC detected with ^{31}P-MRS together resulted in a significant decrease ($P \leq$

335   0.04) in tCho levels (Figure 1D). Furthermore, significant decreases ($P \leq 0.05$) in

336   lactate, alanine, glutamine, glutathione, creatine (Cr) and PCr levels were detected

337   over the time course of treatment (Figure 1E). A significant ($P \leq 0.05$) decrease in

338   glutamate and increase in glucose were also found following 24 h of MK-2206

339   treatment (Figure 1E). We also assessed the metabolic effects of MK-2206 at a lower

340   concentration equivalent to $3 \times GI_{50}$ for 24 h. This resulted in inhibition of AKT

341   signalling and cellular growth (down to $84 \pm 8\%$, $P = 0.008$) as well as a G1 cell cycle

342   arrest compared to controls, but did not induce apoptosis as detemined by cleaved

343   PARP (Supplementary Figure S1A). ^{31}P-MRS showed similar changes in PC, PE, PCr

344   and NTP to those observed with MK-2206 at $5 \times GI_{50}$, but levels of GPE and GPC

345   were not affected (Table 1). Similarly, decreases in PC, tCho, lactate, alanine,

346   glutathione, Cr and PCr were detected using ^{1}H-MRS, while glutamate, glutamine and

347   glucose levels remained unchanged relative to controls (Supplementary Figure S1B

348   and C).

349

350   ***In vitro* investigation of molecular and metabolic effects of treatment with MK-**

351   **2206 in HT29 human colon cancer cells.** To test for the generality of the MRS-

352   detected data, we also treated *PIK3CA* mutant HT29 colorectal carcinoma cells with

353   MK-2206 at $5 \times GI_{50}$ ($GI_{50} = 0.4$ μM) for 24 h. Similar to PC3 prostate cells, treatment

354   with MK-2206 resulted in inhibition of AKT signalling and a G1 cell cycle arrest but

355   no effects on cell number nor apoptosis were detected relative to controls

356   (Supplementary Figure S2A and B). Representative [31]P- and [1]H-MR spectra are

357   shown in Supplementary Figure S2C. As in PC3 cells, ^{31}P-MRS analysis showed

358   significant decreases ($P \leq 0.04$) in PE, PC, PCr and NTP and increases in GPE and

359   GPC in spectra from MK-2206 treated cells compared to their controls (Table 1). [1]H-

360   MRS confirmed changes in PC, GPC and further showed a reduction in tCho

361   (Supplementary Figure S2D). Consistent with PC3 cells, significant decreases ($P \leq$

15

362   0.04) in lactate, alanine, glutamate, glutamine, glutathione, Cr and PCr were also

363   observed in HT29 cells following MK-2206 treatment (Supplementary Figure S2E).

364   In contrast to PC3 cells, treatment with MK-2206 reduced glucose levels in HT29

365   cells ($P < 0.02$; Supplementary Figure S2E).

366

367   **Assessment of mechanisms underlying the *in vitro* MRS detected metabolic**

368   **changes following treatment with MK-2206**. We have used immunoblotting to

369   identify the effects of AKT inhibition with MK-2206 on enzymes involved in choline

370   and glucose metabolism. A decrease in choline kinase alpha (CHKA) expression

371   levels compared to control cells was observed over the time course of treatment with

372   MK-2206 in PC3 and following 24 h treatment with MK-2206 in HT29 cells

373   (Supplementary Figure S3A and B). For the glycolytic metabolic changes, reductions

374   in the protein expression levels of the glycolytic enzymes including hexokinase II

375   (HK2) and lactate dehydrogenase alpha (LDHA) were detected in both cell lines

376   following treatment with MK-2206 (Supplementary Figure S3A and B).

377

378   Next, in order to determine whether the changes in intracellular metabolites

379   could be due to alterations in metabolic flux, we used ^{1}H-MRS to measure levels of

380   metabolites in the growth media of control and treated cells. In the PC3 cells

381   (Supplementary Figure S4A), treatment with MK-2206 ($5xGI_{50}$) caused no significant

382   changes in external metabolites at 6 h compared to controls. However, significant

383   increases ($P < 0.05$) in the levels of alanine, glutamine and choline were observed at

384   12 h following treatment. High levels of all metabolites were detected in growth

385   media of 24 h treated cells compared to controls resulting from the release of

386   metabolites from fragmented apoptotic cells. In contrast, 24 h treatment with MK-

16

387   2206 at 3xGI$_{50}$ only caused a significant increase ($P = 0.01$) in the level of choline

388   compared to controls. Increases in the levels of metabolites present in the growth

389   media from HT29 cells treated with MK-2206 (5xGI$_{50}$) were detected but did not

390   reach significance relative to controls (Supplementary Figure S4B).

391

392   ***In vivo* investigation of molecular and metabolic effects of treatment with MK-**

393   **2206 in subcutaneous HT29 colon xenografts.** Significant tumour growth inhibition

394   was observed in HT29 xenografts after 2 doses (Day 1 and 3) of MK-2206 (120

395   mg/kg per dose) when compared with vehicle-treated controls (Figure 2A). AKT

396   inhibition was confirmed by reductions in the phosphorylation of P70S6K, RPS6

397   (Ser235/236), AKT (Ser473) and AKT (Thr308; Supplementary Figure S5). *In vivo*

398   ^{1}H-MRS showed a significant decrease ($P = 0.04$) in the ratio of tCho/water signal in

399   HT29 xenografts after MK-2206 treatment (Table 2). The *in vivo* change in

400   tCho/water was confirmed by lower PC, GPC and GPE levels in *ex vivo* ^{31}P-MRS

401   analysis of MK-2206 treated tumour extracts when compared with vehicle controls

402   (Table 2). Lower levels of glutamine, glutamate, aspartate, glycine, glutathione and Cr

403   were also seen in MK-2206 treated tumours when compared with controls (Table 2).

404   Phosphocreatine, ATP+ADP, NTP [0.68 ± 0.07 (control) versus 0.48 ± 0.03 (MK-

405   2206) µmol/g wet weight; $P = 0.015$] and NDP [0.49 ± 0.02 (control) versus $0.30 \pm$

406   0.02 (MK-2206) µmol/g wet weight; $P = 0.0004$] levels were also found to reduce in

407   the MK-2206 treated group (Table 2). No change in glucose and lactate levels,

408   microvessel density, necrosis, proliferation or apoptosis was found in MK-2206

409   treated   HT29   tumours   when   compared   to   vehicle   controls   using

410   immunohistochemistry.

411

***In vivo* investigation of molecular and metabolic effects of treatment with MK-2206 in subcutaneous PC3 prostate tumour xenografts.** Similar to MK-2206 treated HT29 xenografts, significant tumour growth inhibition was also observed in PC3 xenografts after 2 doses (Day 1 and 3) of MK-2206 (120 mg/kg per dose) when compared with vehicle-treated controls (Figure 2B) and AKT inhibition was confirmed by the reductions in the phosphorylation of P70S6K, RPS6 (Ser235/236), AKT (Ser473) and AKT (Thr308) (Supplementary Figure S6). *In vivo* ^{1}H-MRS did not show a change in the ratio of tCho/water signal in either control or MK-2206 treated PC3 xenografts (Table 3). However, a significant increase ($P = 0.02$) in the ratio of PMEs/total P signal was found in MK-2206 treated PC3 xenografts by *in vivo* ^{31}P-MRS (Table 3), with this *in vivo* change attributable to a significant increase ($P = 0.03$) in PE measured by ^{31}P-MRS of MK-2206 treated PC3 tumour extracts (Table 3). Significant decreases ($P \leq 0.04$) in GPC, GPE and lactate and increase in glutamine were also found in MK-2206 treated PC3 tumour extracts when compared with vehicle controls (Table 3). No change in tumour bioenergetics was observed in this tumour model following MK-2206 treatment. Immunohistochemical analysis (Figure 2C) on the tumour samples showed significantly decreased microvessel density (CD31) in MK-2206 treated tumours (9 ± 2 stained blood vessels average over 3 fields) when compared to vehicle-controls (14 ± 2; $P = 0.05$). Using immunohistochemistry, no change in necrosis, proliferation or apoptosis was found in MK-2206 treated tumours when compared to controls (Figure 2C).

***In vivo* investigation of molecular and metabolic effects of treatment with MK-2206 in orthotopic PC3 prostate xenografts.** Next we wanted to examine the metabolic response to MK-2206 in a more clinically relevant *in vivo* model.

18

437   Orthotopic PC3 tumours were propagated, treated with MK-2206 (2 doses of 120

438   mg/kg on Day 1 and 3) and studied by ^{1}H-MRS. AKT inhibition was confirmed by

439   the reductions in phosphorylated RPS6 (Ser240/244), AKT (Ser473) and AKT

440   (Thr308; Supplementary Figure S7). *In vivo* ^{1}H-MRS showed that the tCho/water

441   ratio was significantly reduced ($P = 0.02$) in orthotopic PC3 tumours after MK-2206

442   treatment, with this reduction attributable to a significant decrease ($P = 0.003$) in PC

443   as measured *ex vivo* by ^{31}P-MRS analysis of the tumour extracts (Table 4). Significant

444   decreases ($P \leq 0.03$) in alanine and increases in glucose were also found in MK-2206

445   treated tumours (Table 4). No changes in tumour bioenergetics, glutamine or

446   glutathione metabolism were observed in this tumour model following MK-2206

447   treatment. No change in microvessel density, necrosis, proliferation or apoptosis was

448   found in MK-2206 treated tumours when compared to vehicle-controls.

449

Discussion

450

451   AKT is a central component of the PI3K signalling pathway, influencing

452   multiple processes that are directly involved in tumorigenesis. Targeting AKT is

453   therefore a highly attractive anti-cancer strategy and several AKT inhibitors are

454   currently in different phases of clinical trials (Brown and Banerji, 2017; Khan *et al*,

455   2013; Nitulescu *et al*, 2016). As with most cancer targeted therapy, AKT inhibitors

456   were shown to cause anti-proliferative, rather than anti-tumour activity, with stable

457   disease identified as the best overall response (Ahn *et al*, 2015; Yap *et al*, 2011; Yap

458   *et al*, 2014). Therefore, the use of conventional, anatomically based end-points such

459   as RECIST is inadequate (Serkova and Eckhardt, 2016; Teng *et al*, 2013). AKT also

460   plays a pivotal role in the metabolic reprogramming of cancer, providing a rationale

461   for the use of non-invasive functional imaging techniques (such as MRS or PET) as

462   alternative methods to monitor response to this targeted therapy (Beloueche-Babari *et*

463   *al*, 2010; Beloueche-Babari *et al*, 2011; Moestue *et al*, 2011; Serkova and Eckhardt,

464   2016; Workman *et al*, 2006).

465

466   We used MRS both *in vitro* and *in vivo* to identify whether inhibition of AKT

467   signalling using the allosteric pan-AKT inhibitor MK-2206 would result in metabolic

468   changes that can potentially be used to monitor response to AKT inhibition in clinical

469   trials. We performed our investigation using the human *PIK3CA* mutant colorectal

470   carcinoma HT29 and PTEN null prostate carcinoma PC3 cancer models as AKT

471   signalling is involved in the tumorigenesis of colorectal and prostate cancers and AKT

472   inhibitors are in clinical evaluation for both cancer types (Agarwal *et al*, 2013; Toren

473   and Zoubeidi, 2014; Yap *et al*, 2016).

474

475   MK-2206 consistently resulted in the reduction of AKT and its downstream,

476   mTOR, signalling pathways in PC3 and HT29 cells and tumours confirming the

477   mechanism of action.

478

479   Treatment of PC3 cells with MK-2206 resulted in decreases in PE, PC, tCho,

480   lactate, alanine, glutamine, glutathione, Cr, PCr and NTP levels from 6 h post-

481   treatment onwards which was associated with AKT/mTOR pathway inhibition, but

482   was much earlier than the G1 arrest, induction of apoptosis and the decrease in

483   proliferation which were only evident at 24 h following treatment with MK-2206.

484   This indicates that our detected metabolic changes are related to the inhibition of

485   AKT/mTOR signalling rather than to the anti-proliferative effects of the treatment. In

486   support of previous reports by ourselves and others using PI3K/mTOR/AKT

487   inhibitors (Al-Saffar *et al*, 2010; Al-Saffar *et al*, 2014; Chaumeil *et al*, 2012; Su *et al*,

488   2012; Venkatesh *et al*, 2012), the decrease in PC levels following MK-2206 treatment

489   was associated with a decrease in the protein levels of CHKA, the enzyme responsible

490   for choline phosphorylation to form PC. A decrease in the protein expression levels of

491   the glycolytic enzymes HK2 and LDHA were also observed following AKT

492   inhibition, suggesting mechanisms for the depletion of lactate. Higher levels of

493   choline were also found in the tissue culture media of cells treated with MK-2206

494   compared to controls indicating inhibition of uptake as another mechanism for the

495   decrease in intracellular levels of PC. Furthermore, decreased intracellular and

496   increased extracellular levels of alanine indicate the conversion of pyruvate into

497   alanine instead of lactate as a result of inhibition of LDHA and increased eflux of

498   alanine following treatment with MK-2206. A decrease in the intracellular and

499   increase in the extracellular level of glutamine was also detected in treated cells which

500 maybe related to decreased uptake of glutamine into the cells following MK-2206

501 treatment.

502

503   Treatment with MK-2206 also reduced levels of GPE and GPC for up to 12 h

504 but then an increase was observed at 24 h. The later increase in GPE and GPC might

505 be linked to the apoptotic effects of MK-2206 observed at this time point which

506 would lead to membrane breakdown and remodeling (Morse *et al*, 2007; Zhang *et al*,

507 2018). We have previously observed an increase in GPC following treatment with

508 some PI3K inhibitors but that was cell line dependent and, moreover, was seen only

509 after longer inhibition periods ($\geq$ 16 h) and when higher concentrations ($5xGI_{50}$) of

510 PI3K pathway inhibitors were used (Al-Saffar *et al*, 2010; Al-Saffar *et al*, 2014;

511 Beloueche-Babari *et al*, 2006). This was further supported by our findings that when

512 we used MK-2206 at a concentration equivalent to $3xGI_{50}$. This concentration did not

513 cause apoptosis and had no effects on GPC or GPE levels.

514

515   Similar to PC3 cells, metabolic changes including reductions in PE, PC, tCho,

516 lactate, alanine, glutamate, glutamine, glutathione, Cr and PCr as well as an increase

517 in GPE and GPC were detected following treatment of HT29 colorectal carcinoma

518 cells with MK-2206 at $5xGI_{50}$ for 24 h. This was associated with inhibition of

519 AKT/mTOR signalling and a G1 cell cycle arrest. The observed changes in

520 phospholipid and glucose metabolism are congruent with the previous reports

521 examining the effect of the AKT inhibitors perifosine and MK-2206 on breast cancer

522 cells (Phyu *et al*, 2016; Su *et al*, 2012), and suggest that choline-containing

523 metabolites and lactate may serve as non-invasive metabolic biomarkers for

524 monitoring the effects of AKT inhibitors.

525

Similar phospholipid and glutamine changes to those detected in HT29 cells were also observed in HT29 xenografts following treatment with MK-2206. These were associated with a significant tumour growth delay and pathway inhibition when compared with vehicle-treated controls. *In vivo* ^{1}H-MRS analysis of the HT29 tumour xenografts showed a significant decrease in the ratio of tCho/water signal. This was further confirmed by significantly lower PC, GPC and GPE levels by *ex vivo* ^{31}P-MRS of MK-2206 treated tumour extracts when compared with vehicle controls, supporting the *in vitro* findings and suggesting that membrane turnover is reduced following MK-2206 treatment. Tumour bioenergetics was also compromised by treatment with MK-2206 as indicated by the decrease in the levels of PCr, ATP+ADP, NTP and NDP. Consistent with our *in vitro* cell data, alterations in glutamine and glutathione metabolism with decreased glutamine, glutamate, aspartate, glutathione, glycine and Cr were also found in HT29 tumours following AKT inhibition with MK-2206. No change in glucose metabolism was observed in MK-2206 treated HT29 xenografts.

Glutamine is one of the key substrates utilised by cancer cells and its metabolism is important to tumour growth, malignancy, and survival under stress (Hensley *et al*, 2013). Glutamine is involved in nucleotide synthesis (Cory and Cory, 2006), and generation of the anti-oxidant glutathione (Shanware *et al*, 2011). The decreases in bioenergetic metabolites, such as nucleotides and PCr following MK-2206 treatment are consistent with the observed decreases in glycine, glutamine and its downstream metabolites, such as glutamate, aspartate and Cr, suggesting that lower

549 tumour bioenergetics following treatment maybe a consequence of changes in

550 glutamine metabolism.

551

552   Our data also indicate that glutathione biosynthesis may be altered following

553 MK-2206 treatment, as the total glutathione level together with its precursors,

554 glutamine and glycine, were lower in the MK-2206 treated PC3 and HT29 cells and

555 tumours. This is consistent with previous reports that glutathione levels are reduced in

556 MK-2206 treated lung cancer cells (Dai *et al*, 2013) and that the PI3K/AKT signalling

557 pathway in *PIK3CA* mutant and *PTEN* mutant breast cancer cells stimulates

558 glutathione biosynthesis, in order to counteract the effect of oxidative stress (Lien *et*

559 *al*, 2016).

560

561   Different changes in PC levels have been previously reported following

562 treatment with MK-2206 in MDA-MB-468 breast cancer cells (Phyu *et al*, 2016)

563 compared to basal like breast cancer tumours (Moestue *et al*, 2013). This was the case

564 with MK-2206 treated subcutaneous PC3 xenografts, where in contrast to PC3 cells,

565 an increase rather than a decrease in the ratio of PMEs/total P signal was observed by

566 *in vivo* ^{31}P-MRS, and no significant difference in the tCho/water ratio was detected by

567 *in vivo* ^{1}H-MRS pre vs. post MK-2206 treatment. Further investigations using *ex vivo*

568 MRS showed an increase in PE and a decrease in GPC and GPE in MK-2206 treated

569 subcutaneous PC3 tumour extracts when compared with vehicle controls. These

570 changes in choline and ethanolamine metabolites could explain the lack of change in

571 the *in vivo* MRS detected tCho/water signal as it consists of PC, PE, GPC and GPE,

572 and the increase in PMEs consisting of PC and PE.

573

574   Differences in phospholipid metabolism between PC3 cells in culture and in

575   subcutaneous tumours derived from these cells have been previously reported and was

576   attributed to the influence of the tumour microenvironment on choline and lipid

577   metabolism (Mori *et al*, 2016). However, our MRS detected phospholipid changes

578   observed in the colorectal HT29 subcutaneous tumours are consistent with our *in vitro*

579   findings both in HT29 and PC3 cells and also in line with the previously published

580   MRS changes using the AKT inhibitors perifosine and MK-2206 in breast cancer cells

581   (Phyu *et al*, 2016; Su *et al*, 2012). We also did not observe any differences in the

582   cellular or molecular effects of MK-2206 in both tumour models. We therefore

583   questioned whether the difference in the phospholipid biomarker changes in the PC3

584   subcutaneous tumours was due to the location of the tumour, and whether growing

585   PC3 tumours orthotopically would result in a different metabolic response to

586   treatment with the AKT inhibitor MK-2206 compared to PC3 subcutaneous tumours.

587   Orthotopic tumour models are more clinically relevant compared to subcutaneous

588   tumours. A previous study showed images in real time, using green fluorescent

589   protein (GFP) expression, of the very different tumour behaviour at the orthotopic and

590   subcutaneous sites of human prostate cancer PC3 in athymic nude mice. The

591   orthotopic tumour described had higher rates of vascularisation, migration,

592   angiogenesis and metastasis compared to the subcutaneous tumour (Zhang *et al*,

593   2016). Indeed, inhibition of AKT signalling with MK-2206 in orthotopic PC3

594   tumours resulted in a significant reduction in the tCho/water ratio using *in vivo* [1]H-

595   MRS and this was due to a decrease in PC levels as shown in the MRS analysis of the

596   tumour extracts. Similar to MK-2206 treated PC3 and HT29 cells, orthotopic PC3

597   tumours treated with MK-2206 also showed reduced alanine and increased glucose,

598   suggesting an alteration in glucose metabolism. MK-2206 had no effect on tumour

599   bioenergetics, glutamine or glutathione metabolism, microvessel density, necrosis,

600   proliferation or apoptosis. This shows that the difference in metabolic response

601   between subcutaneous and orthotopic PC3 tumours could reflect the difference in

602   tumour microenvironment at different tumour sites.

603

604   We have provided further evidence that *in vitro* inhibition of AKT is associated

605   with changes in glucose, glutamine and choline metabolism both in prostate and

606   colorectal cancer cell lines. We also demonstrated that the reduction in choline

607   metabolites can be detected *in vivo* both in subcutaneous and the clinically relevant

608   orthotopic prostate cancer tumours. A Phase I trial study published previously

609   investigated the utility of ^{1}H-MRS (amongst a number of functional imaging

610   biomarkers) to monitor patient response to MK-2206 (Yap *et al*, 2014). Individual but

611   not cohort ^{1}H-MRS detected changes in tCho/water ratio have been reported. This

612   was possibly due to insufficient target and pathway modulation as the ultimate

613   maximum tolerated dose (MTD) was limited by Dose Limiting Toxicities (DLTs) of

614   rash during dose escalation. The Phase I study also involved a very small population

615   of patients. The authors suggested that functional imaging studies including total

616   choline levels should be considered in phase II trials using a higher dose of MK-2206.

617   Taken together, our MRS-detected choline metabolites may have potential as

618   non-invasive biomarkers for monitoring response to treatment with AKT inhibitors

619   during Phase I/II clinical trials in selected cancer types.

620

621 **Additional Information:**

622

623 **Ethics approval**

624 All animal experiments were performed in accordance with local and national ethical

625 review panel, the UK Home Office Animals (Scientific Procedures) Act 1986 and the

626 United Kingdom Coordinating Committee on Cancer Research Guidelines for the

627 Welfare of Animals in Experimental Neoplasia (Workman et al. *BJC* 2010)

628

629 **Availability of data and material**

630 All data generated or analysed during this study are included in this published article

631 and its supplementary information files.

632

633 **Conflict of interest.**

634 The authors declare no conflict of interest.

635

636 **Funding**

637 This work is funded by Cancer Research UK and EPSRC Cancer Imaging Centre in

638 association with the MRC and Department of Health (England) grant C1060/A10334

639 and C1060/A16464 for M.O.L, Y-L.C, N.M.S.A, A.C.W.T.F, R.P., S.P.R, J.K.R.B,

640 and L.E.J. M.O.L is an Emeritus NIHR Senior Investigator. All authors acknowledge

641 National Health Service funding to the NIHR Biomedical Research Centre.

642

643 **Authors' contributions**

644 NMSA and Y-LC wrote the manuscript text. NMSA, Y-LC, TAY and MOL

645 conceived the study. NMSA, Y-LC, HT, LEJ, ACWTF, SG, RP and JKRB designed

646   and performed experiments. NMSA, Y-LC, ACWTF and SG analysed the data.

647   NMSA, Y-LC, SPR, SAE and MOL contributed reagents/ materials/analysis tools. All

648   authors reviewed the manuscript.

653

654   Supplementary information is available at the British Journal of Cancer's website

655

656   **References**

657   Agarwal, E., Brattain, M. G., and Chowdhury, S. (2013). Cell survival and metastasis

658   regulation by Akt signaling in colorectal cancer. Cell Signal *25*, 1711-1719.

659   Ahn, D. H., Li, J., Wei, L., Doyle, A., Marshall, J. L., Schaaf, L. J., Phelps, M. A.,

660   Villalona-Calero, M. A., and Bekaii-Saab, T. (2015). Results of an abbreviated phase-

661   II study with the Akt Inhibitor MK-2206 in Patients with Advanced Biliary Cancer.

662   Sci Rep *5*, 12122.

663   Al-Saffar, N. M., Jackson, L. E., Raynaud, F. I., Clarke, P. A., Ramírez de Molina, A.,

664   Lacal, J. C., Workman, P., and Leach, M. O. (2010). The Phosphoinositide 3-Kinase

665   Inhibitor PI-103 Downregulates Choline Kinase {alpha} Leading to Phosphocholine

666   and Total Choline Decrease Detected by Magnetic Resonance Spectroscopy. Cancer

667   Res *70*, 5507-5517.

668   Al-Saffar, N. M., Marshall, L. V., Jackson, L. E., Balarajah, G., Eykyn, T. R.,

669   Agliano, A., Clarke, P. A., Jones, C., Workman, P., Pearson, A. D., and Leach, M. O.

670   (2014). Lactate and choline metabolites detected in vitro by nuclear magnetic

671   resonance spectroscopy are potential metabolic biomarkers for PI3K inhibition in

672   pediatric glioblastoma. PLoS One *9*, e103835.

673   Beloueche-Babari, M., Chung, Y. L., Al-Saffar, N. M., Falck-Miniotis, M., and

674   Leach, M. O. (2010). Metabolic assessment of the action of targeted cancer

675   therapeutics using magnetic resonance spectroscopy. BrJCancer *102*, 1-7.

676   Beloueche-Babari, M., Jackson, L. E., Al-Saffar, N. M. S., Eccles, S. A., Raynaud, F.

677   I., Workman, P., Leach, M. O., and Ronen, S. M. (2006). Identification of magnetic

678   resonance detectable metabolic changes associated with inhibition of

679   phosphoinositide 3-kinase signaling in human breast cancer cells. Molecular Cancer

680   Therapeutics *5*, 187-196.

681   Beloueche-Babari, M., Workman, P., and Leach, M. O. (2011). Exploiting tumor

682   metabolism for non-invasive imaging of the therapeutic activity of molecularly

683   targeted anticancer agents. Cell Cycle *10*, 2883-2893.

684   Bosari, S., Lee, A. K., DeLellis, R. A., Wiley, B. D., Heatley, G. J., and Silverman,

685   M. L. (1992). Microvessel quantitation and prognosis in invasive breast carcinoma.

686   Hum Pathol *23*, 755-761.

687   Brown, J. S., and Banerji, U. (2017). Maximising the potential of AKT inhibitors as

688   anti-cancer treatments. Pharmacol Ther *172*, 101-115.

689   Chaumeil, M. M., Ozawa, T., Park, I., Scott, K., James, C. D., Nelson, S. J., and

690   Ronen, S. M. (2012). Hyperpolarized 13C MR spectroscopic imaging can be used to

691   monitor Everolimus treatment in vivo in an orthotopic rodent model of glioblastoma.

692   Neuroimage *59*, 193-201.

693   Chung, Y. L. (2017). Magnetic Resonance Spectroscopy (MRS)-Based Methods for

694   Examining Cancer Metabolism in Response to Oncogenic Kinase Drug Treatment.

695   Methods Mol Biol *1636*, 393-404.

696   Cory, J. G., and Cory, A. H. (2006). Critical roles of glutamine as nitrogen donors in

697   purine and pyrimidine nucleotide synthesis: asparaginase treatment in childhood acute

698   lymphoblastic leukemia. In Vivo *20*, 587-589.

699   Dai, B., Yoo, S. Y., Bartholomeusz, G., Graham, R. A., Majidi, M., Yan, S., Meng, J.,

700   Ji, L., Coombes, K., Minna, J. D. *et al* (2013). KEAP1-dependent synthetic lethality

701   induced by AKT and TXNRD1 inhibitors in lung cancer. Cancer Res *73*, 5532-5543.

702   Esmaeili, M., Bathen, T. F., Engebraten, O., Maelandsmo, G. M., Gribbestad, I. S.,

703   and Moestue, S. A. (2014). Quantitative (31)P HR-MAS MR spectroscopy for

704   detection of response to PI3K/mTOR inhibition in breast cancer xenografts. Magnetic

705   resonance in medicine : official journal of the Society of Magnetic Resonance in

706   Medicine / Society of Magnetic Resonance in Medicine *71*, 1973-1981.

707   Euceda, L. R., Hill, D. K., Stokke, E., Hatem, R., El Botty, R., Bieche, I., Marangoni,

708   E., Bathen, T. F., and Moestue, S. A. (2017). Metabolic Response to Everolimus in

709   Patient-Derived Triple-Negative Breast Cancer Xenografts. J Proteome Res *16*, 1868-

710   1879.

711   Gadian, D. G. (1995). The information available from NMR. In NMR and its

712   applications to living systems, (New York: Oxford University Press Inc.), pp. 29-64.

713   Hanahan, D., and Weinberg, R. A. (2011). Hallmarks of cancer: the next generation.

714   Cell *144*, 646-674.

715   Hensley, C. T., Wasti, A. T., and DeBerardinis, R. J. (2013). Glutamine and cancer:

716   cell biology, physiology, and clinical opportunities. J Clin Invest *123*, 3678-3684.

717   Iurlaro, R., Leon-Annicchiarico, C. L., and Munoz-Pinedo, C. (2014). Regulation of

718   cancer metabolism by oncogenes and tumor suppressors. Methods Enzymol *542*, 59-

719   80.

720   Khan, K. H., Yap, T. A., Yan, L., and Cunningham, D. (2013). Targeting the PI3K-

721   AKT-mTOR signaling network in cancer. Chin J Cancer *32*, 253-265.

722   Koul, D., Shen, R., Kim, Y. W., Kondo, Y., Lu, Y., Bankson, J., Ronen, S. M.,

723   Kirkpatrick, D. L., Powis, G., and Yung, W. K. (2010). Cellular and in vivo activity

724   of a novel PI3K inhibitor, PX-866, against human glioblastoma. NeuroOncol.

725   Lee, S. C., Marzec, M., Liu, X., Wehrli, S., Kantekure, K., Ragunath, P. N., Nelson,

726   D. S., Delikatny, E. J., Glickson, J. D., and Wasik, M. A. (2013). Decreased lactate

727   concentration and glycolytic enzyme expression reflect inhibition of mTOR signal

728   transduction pathway in B-cell lymphoma. NMR Biomed *26*, 106-114.

729 Lien, E. C., Lyssiotis, C. A., Juvekar, A., Hu, H., Asara, J. M., Cantley, L. C., and

730 Toker, A. (2016). Glutathione biosynthesis is a metabolic vulnerability in PI(3)K/Akt-

731 driven breast cancer. Nat Cell Biol *18*, 572-578.

732 Manning, B. D., and Toker, A. (2017). AKT/PKB Signaling: Navigating the Network.

733 Cell *169*, 381-405.

734 Moestue, S. A., Dam, C. G., Gorad, S. S., Kristian, A., Bofin, A., Maelandsmo, G.

735 M., Engebraten, O., Gribbestad, I. S., and Bjorkoy, G. (2013). Metabolic biomarkers

736 for response to PI3K inhibition in basal-like breast cancer. Breast Cancer Res *15*,

737 R16.

738 Moestue, S. A., Engebraaten, O., and Gribbestad, I. S. (2011). Metabolic effects of

739 signal transduction inhibition in cancer assessed by magnetic resonance spectroscopy.

740 Mol Oncol *5*, 224-241.

741 Mori, N., Wildes, F., Takagi, T., Glunde, K., and Bhujwalla, Z. M. (2016). The

742 Tumor Microenvironment Modulates Choline and Lipid Metabolism. Front Oncol *6*,

743 262.

744 Morse, D. L., Galons, J. P., Payne, C. M., Jennings, D. L., Day, S., Xia, G., and

745 Gillies, R. J. (2007). MRI-measured water mobility increases in response to

746 chemotherapy via multiple cell-death mechanisms. NMR Biomed *20*, 602-614.

747 Nitulescu, G. M., Margina, D., Juzenas, P., Peng, Q., Olaru, O. T., Saloustros, E.,

748 Fenga, C., Spandidos, D., Libra, M., and Tsatsakis, A. M. (2016). Akt inhibitors in

749 cancer treatment: The long journey from drug discovery to clinical use (Review). Int J

750 Oncol *48*, 869-885.

751 Pavlova, N. N., and Thompson, C. B. (2016). The Emerging Hallmarks of Cancer

752 Metabolism. Cell Metab *23*, 27-47.

33

753   Phyu, S. M., Tseng, C. C., Fleming, I. N., and Smith, T. A. (2016). Probing the

754   PI3K/Akt/mTor pathway using (31)P-NMR spectroscopy: routes to glycogen synthase

755   kinase 3. Sci Rep *6*, 36544.

756   Raynaud, F. I., Eccles, S., Clarke, P. A., Hayes, A., Nutley, B., Alix, S., Henley, A.,

757   Di-Stefano, F., Ahmad, Z., Guillard, S. *et al* (2007). Pharmacologic characterization

758   of a potent inhibitor of class I phosphatidylinositide 3-kinases. Cancer Research *67*,

759   5840-5850.

760   Serkova, N. J., and Eckhardt, S. G. (2016). Metabolic Imaging to Assess Treatment

761   Response to Cytotoxic and Cytostatic Agents. Front Oncol *6*, 152.

762   Shanware, N. P., Mullen, A. R., DeBerardinis, R. J., and Abraham, R. T. (2011).

763   Glutamine: pleiotropic roles in tumor growth and stress resistance. J Mol Med (Berl)

764   *89*, 229-236.

765   Sitter, B., Sonnewald, U., Spraul, M., Fjosne, H. E., and Gribbestad, I. S. (2002).

766   High-resolution magic angle spinning MRS of breast cancer tissue. NMR Biomed *15*,

767   327-337.

768   Su, J. S., Woods, S. M., and Ronen, S. M. (2012). Metabolic consequences of

769   treatment with AKT inhibitor perifosine in breast cancer cells. NMR Biomed *25*, 379-

770   388.

771   Tarrado-Castellarnau, M., de Atauri, P., and Cascante, M. (2016). Oncogenic

772   regulation of tumor metabolic reprogramming. Oncotarget *7*, 62726-62753.

773   Teng, F. F., Meng, X., Sun, X. D., and Yu, J. M. (2013). New strategy for monitoring

774   targeted therapy: molecular imaging. Int J Nanomedicine *8*, 3703-3713.

775   Toren, P., and Zoubeidi, A. (2014). Targeting the PI3K/Akt pathway in prostate

776   cancer: challenges and opportunities (review). Int J Oncol *45*, 1793-1801.

777 Tyagi, R. K., Azrad, A., Degani, H., and Salomon, Y. (1996). Simultaneous extraction

778 of cellular lipids and water-soluble metabolites: Evaluation by NMR spectroscopy.

779 Magnetic Resonance in Medicine *35*, 194-200.

780 Venkatesh, H. S., Chaumeil, M. M., Ward, C. S., Haas-Kogan, D. A., James, C. D.,

781 and Ronen, S. M. (2012). Reduced phosphocholine and hyperpolarized lactate provide

782 magnetic resonance biomarkers of PI3K/Akt/mTOR inhibition in glioblastoma.

783 NeuroOncol *14*, 315-325.

784 Workman, P., Aboagye, E. O., Balkwill, F., Balmain, A., Bruder, G., Chaplin, D. J.,

785 Double, J. A., Everitt, J., Farningham, D. A., Glennie, M. J. *et al* (2010). Guidelines

786 for the welfare and use of animals in cancer research. Br J Cancer *102*, 1555-1577.

787 Workman, P., Aboagye, E. O., Chung, Y. L., Griffiths, J. R., Hart, R., Leach, M. O.,

788 Maxwell, R. J., McSheehy, P. M., Price, P. M., and Zweit, J. (2006). Minimally

789 invasive pharmacokinetic and pharmacodynamic technologies in hypothesis-testing

790 clinical trials of innovative therapies. Journal Of The National Cancer Institute *98*,

791 580-598.

792 Yap, T. A., Smith, A. D., Ferraldeschi, R., Al-Lazikani, B., Workman, P., and de

793 Bono, J. S. (2016). Drug discovery in advanced prostate cancer: translating biology

794 into therapy. Nat Rev Drug Discov *15*, 699-718.

795 Yap, T. A., Yan, L., Patnaik, A., Fearen, I., Olmos, D., Papadopoulos, K., Baird, R.

796 D., Delgado, L., Taylor, A., Lupinacci, L. *et al* (2011). First-in-man clinical trial of

797 the oral pan-AKT inhibitor MK-2206 in patients with advanced solid tumors. J Clin

798 Oncol *29*, 4688-4695.

799 Yap, T. A., Yan, L., Patnaik, A., Tunariu, N., Biondo, A., Fearen, I., Papadopoulos,

800 K. P., Olmos, D., Baird, R., Delgado, L. *et al* (2014). Interrogating two schedules of

801 the AKT inhibitor MK-2206 in patients with advanced solid tumors incorporating

802   novel pharmacodynamic and functional imaging biomarkers. Clin Cancer Res *20*,

803   5672-5685.

804   Zhang, Y., Chen, X., Gueydan, C., and Han, J. (2018). Plasma membrane changes

805   during programmed cell deaths. Cell Res *28*, 9-21.

806   Zhang, Y., Toneri, M., Ma, H., Yang, Z., Bouvet, M., Goto, Y., Seki, N., and

807   Hoffman, R. M. (2016). Real-Time GFP Intravital Imaging of the Differences in

808   Cellular and Angiogenic Behavior of Subcutaneous and Orthotopic Nude-Mouse

809   Models of Human PC-3 Prostate Cancer. J Cell Biochem *117*, 2546-2551.

810

811

812 **Figure Legends**

813 **Figure 1. Molecular and metabolic changes caused by treatment with MK-2206**

814 **in PC3 prostate cancer cells.** (**A**) Representative immunoblots showing changes in

815 molecular markers demonstrating AKT inhibition and induction of apoptosis as

816 evidenced by cleaved PARP. β-Actin is used as a loading control. (**B**) Flow cytometry

817 analysis histograms showing cell cycle distribution of cells with vehicle treatment

818 (DMSO, control), or following treatment with MK-2206 ($5xGI_{50}$) at 24 h post

819 treatment, $P < 0.002$ for G1&S phases. (**C**) Representative *in vitro* ^{31}P-MR spectra

820 (left) and expansion of ^{1}H-MR spectra region (1.3-3.3 ppm; right) showing choline–

821 containing metabolites, Cr/PCr, lactate (Lac) and amino acids (Ala = alanine; Glu =

822 glutamate; Gln = glutamine; GSH = glutathione). A summary of ^{1}H-MRS metabolic

823 changes caused by MK-2206 treatment ($5xGI_{50}$, 24 h) of PC3 prostate cancer cells:

824 (**D**) Choline-containing metabolites. (**E**) Amino acids, Cr/PCr and glycolytic

825 intermediates. Results are expressed as %T/C and presented as mean $\pm$ SD, n $\geq$ 5.

826 Statistically significant differences from the control $^{*}P \leq 0.05$, $^{**}P \leq 0.01$; $^{***}P \leq$

827 0.001.

828

829 **Figure 2. Tumour volume and histological changes in subcutaneous tumours**

830 **following MK-2206 treatment.** Percentage change in HT29 (**A**) and subcutaneous

831 PC3 (**B**) tumour volumes (relative to Day 1) following 2 doses (Day 1 and 3) of 120

832 mg/kg of MK-2206 on alternate days via p.o. (n = 10) or vehicle alone (10% DMSO

833 in saline), minimum n = 10. Data are expressed as mean $\pm$ SEM, ****$P < 0.0001$. (**C**)

834 Immunohistochemistry of Ki67, caspase-3 and CD31 expressions (brown staining) in

835   vehicle-treated control (left column) and MK-2206 treated (right column)

836   subcutaneous PC3 xenografts (right column). Magnification x 200.

837

Table 1. Analysis of ^{31}P-MRS-detected metabolic changes following inhibition with MK-2206 in:									
	PC3								
	6 h (5xGI$_{50}$)	*P*	12 h (5xGI$_{50}$)	*P*	24 h (5xGI$_{50}$)	*P*	24 h (3xGI$_{50}$)	*P*
PE	62 ± 16	0.008	47 ± 11	0.001	23 ± 16	0.0001	43 ± 26	0.01
PC	74 ± 14	0.02	78 ± 11	0.02	69 ± 13	0.001	71 ± 5	0.0004
GPE	66 ± 34	ns	50 ± 12	0.001	320 ± 104	0.005	153 ± 40	ns
GPC	32 ± 16	0.001	36 ± 11	0.0003	225 ± 63	0.007	121 ± 27	ns
PCr	74 ± 28	ns	54 ± 31	0.04	38 ± 24	0.007	46 ± 24	0.01
NTP	63 ± 17	0.01	56 ± 12	0.002	68 ± 18	0.005	82 ± 11	0.03

Data are expressed as %T/C and presented as the mean $\pm$ SD, n $\geq$ 4.
Two-tailed unpaired *t* test was used to compare results in treated cells to controls within the same time-point.

	HT29	
	24 h (5xGI$_{50}$)	*P*
PE	60 ± 9	0.001
PC	67 ± 6	0.0001
GPE	132 ± 26	0.04
GPC	169 ± 31	0.004
PCr	59 ± 8	0.0001
NTP	89 ± 7	0.02

Table 2: *In vivo* and *ex vivo* ^{1}H- and ^{31}P-MRS metabolic analysis of HT29 subcutaneous tumours and extracts following MK-2206 treatment.				
In vivo ^{1}H-MRS of subcutaneous HT29 xenografts				
	Vehicle-Control (n=5)		**MK-2206 (n=5)**	
	Pre-	**Post-**	**Pre**	**Post**
Corrected tCho/water ratio x 10^{-3}	8.05 ± 1.11	6.25 ± 1.84	9.22 ± 1.42	4.33 ±1.03
	P = 0.31		*P* = 0.04	

*Statistically significant when compared the pre-MK-2206 treatment values with post-treatment. Two-tailed paired *t* test was used and data are expressed as mean±sem.

Ex vivo ^{1}H- and ^{31}P-MRS of subcutaneous HT29 tumour extracts			
	Vehicle-Control	**MK-2206**	***p***
PE	1.27 ± 0.10	1.28 ± 0.11	0.96
PC	1.95 ± 0.12	1.60 ± 0.09	0.04*
GPE	1.21 ± 0.14	0.87 ± 0.07	0.03*
GPC	2.51 ± 0.13	1.94 ± 0.18	0.04*
Lactate	5.81 ± 0.58	7.78 ± 0.92	0.10
Alanine	1.49 ± 0.15	1.27 ± 0.08	0.25
Glucose	0.79 ± 0.10	0.70 ± 0.13	0.61
Glutamine	1.01 ± 0.06	0.72 ± 0.02	0.002*
Glutamate	2.67 ± 0.23	1.56 ± 0.30	0.02*
Aspartate	0.35 ± 0.04	0.20 ± 0.05	0.05*
Glycine	0.67 ± 0.11	0.37 ± 0.06	0.04*
Glutathione	1.30 ± 0.11	0.85 ± 0.08	0.007*
Creatine	3.82 ± 0.21	2.87 ± 0.19	0.008*
Phosphocreatine	1.20 ± 0.08	0.74 ± 0.08	0.004*
ATP+ADP	1.38 ± 0.08	1.07 ± 0.07	0.02*

Data are expressed as μmol/g wet weight and presented as the mean±sem, n ≥ 5 in each group. Two-tailed unpaired *t* test was used to compare MK2206-treated tumour extracts with vehicle-treated controls and $^*P$ ≤ 0.05 is considered significant.

Table 3: *In vivo* and *ex vivo* ^{1}H- and ^{31}P-MRS metabolic analysis of subcutaneous PC3 tumours and extracts following MK-2206 treatment.

In vivo ^{1}H- and ^{31}P-MRS of subcutaneous PC3 tumours

	Vehicle-Control		MK-2206	
	Pre-	Post-	Pre-	Post-
Corrected tCho/water ratio x10^{-3} (n = 4 in each group)	3.63 ± 0.38	3.80 ± 0.64	3.26 ± 0.26	3.61 ± 0.17
	P = 0.66		*P* = 0.31	
PME/total P ratio (n = 5 in each group)	0.11 ± 0.01	0.12 ± 0.01	0.14 ± 0.01	0.17 ± 0.02
	P = 0.50		*P* = 0.02	

*Statistically significant when compared the pre-MK-2206 treatment values with post-treatment. Two-tailed paired *t* test was used and data are expressed as mean±sem. PME – phosphomonoesters, total P – total phorphorus signal.

Ex vivo ^{1}H- and ^{31}P-MRS of subcutaneous PC3 tumour extracts			
	Vehicle-Control	MK-2206	*p*
PE	1.03 ± 0.10	1.45 ± 0.13	0.03*
PC	1.53 ± 0.05	1.60 ± 0.20	0.75
GPE	0.44 ± 0.03	0.28 ± 0.04	0.02*
GPC	1.54 ± 0.14	0.94 ± 0.19	0.04*
Lactate	9.34 ± 0.85	7.14 ± 0.44	0.04*
Alanine	1.39 ± 0.13	1.49 ± 0.23	0.74
Glucose	0.45 ± 0.06	0.41 ± 0.03	0.48
Glutamine	1.20 ± 0.16	2.74 ± 0.48	0.02*
Glutamate	3.64 ± 0.41	3.02 ± 0.37	0.28
Glycine	1.21 ± 0.18	1.39 ± 0.16	0.48
Glutathione	1.53 ± 0.15	1.46 ± 0.12	0.74
Creatine	1.08 ± 0.09	1.38 ± 0.24	0.32
Phosphocreatine	0.39 ± 0.05	0.53 ± 0.05	0.08
ATP+ADP	0.84 ± 0.05	0.89 ± 0.07	0.63

Data are expressed as µmol/g wet weight and presented as the mean±sem, n ≥ 5 in each group. Two-tailed unpaired *t* test was used to compare MK2206-treated tumour extracts with vehicle-treated controls and $^*P \leq 0.05$ is considered significant. Aspartate was not detected.

Table 4: *In vivo* and *ex vivo* ^{1}H- and ^{31}P-MRS metabolic analysis of orthotopic PC3 tumours and extracts following MK-2206 treatment.				
In vivo ^{1}H-MRS of orthotopic PC3 tumours				
	Vehicle-Control (n=3)		MK-2206 (n=5)	
	Pre-	Post-	Pre	Post
Corrected tCho/water ratio x10^{-3}	5.11 ± 0.68	4.25 ± 0.47	5.03 ± 0.69	3.92 ± 0.56
	P = 0.36		*P = 0.02	
*Statistically significant when compared the pre-MK-2206 treatment values with post-treatment. Two-tailed paired *t* test was used and data are expressed as mean±sem.				

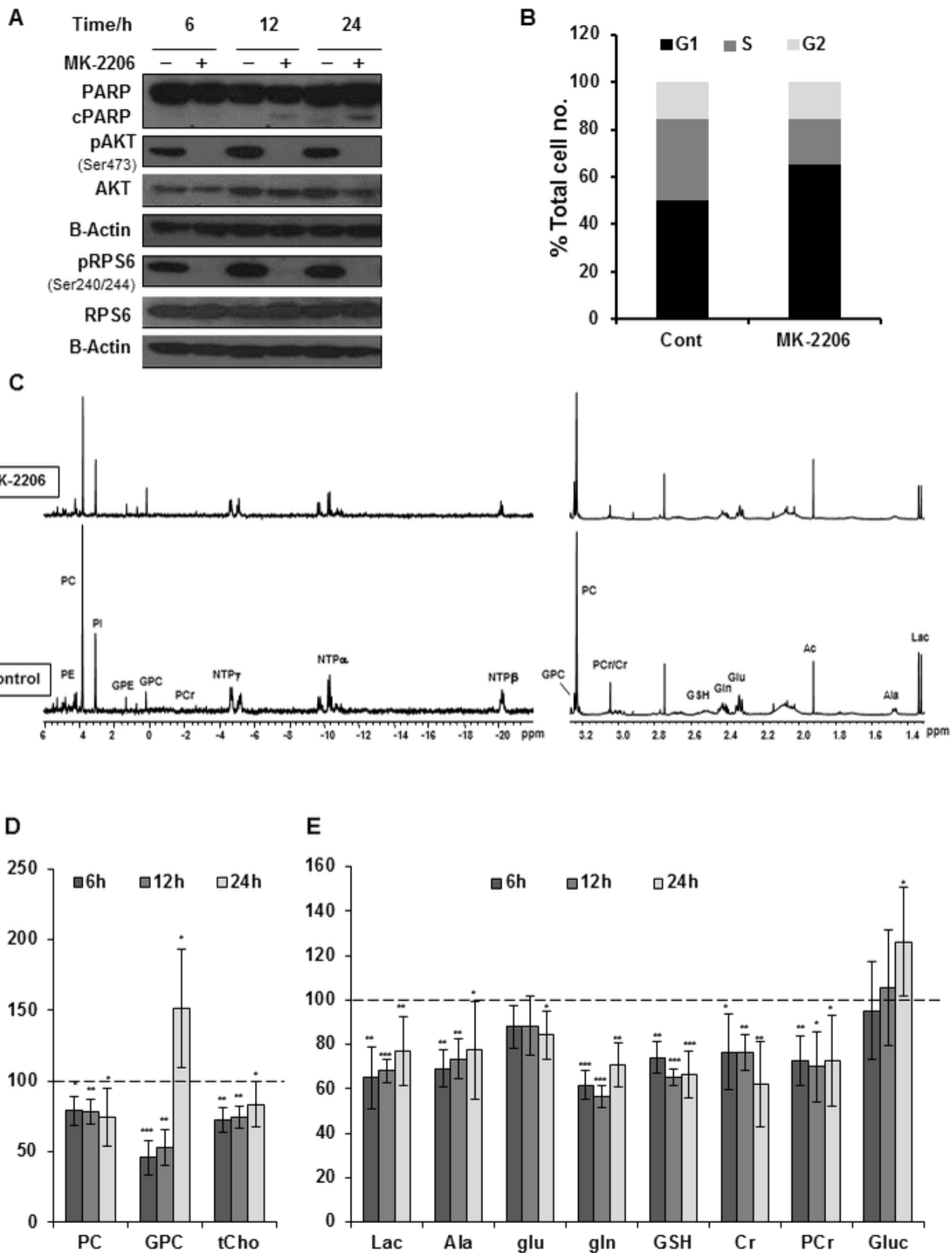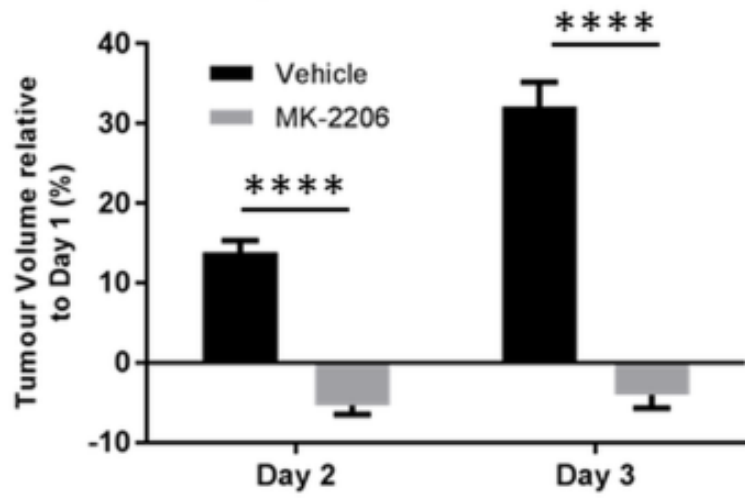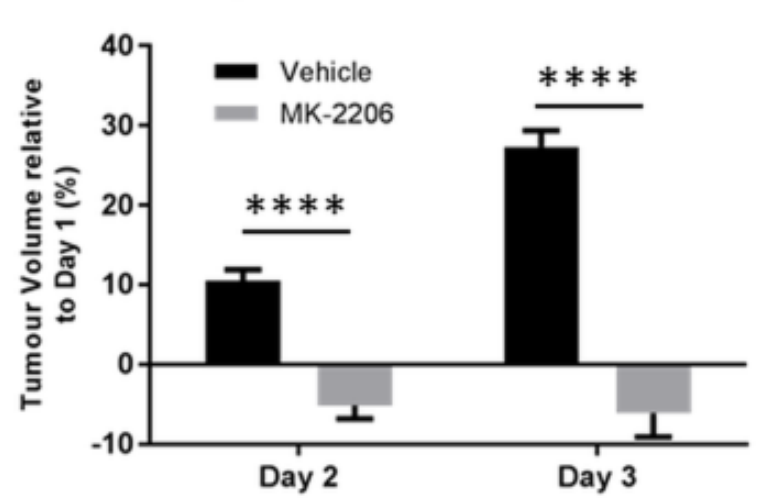| *Ex vivo* ^{1}H- and ^{31}P-MRS of orthotopic PC3 tumour extracts			
	Vehicle-Control	MK-2206	*P*
PE	1.58 ± 0.18	1.20 ± 0.13	0.14
PC	1.80 ± 0.06	1.47 ± 0.06	0.003*
GPE	0.46 ± 0.03	0.45 ± 0.05	0.95
GPC	1.79 ± 0.35	2.16 ± 0.17	0.40
Lactate	5.32 ± 0.65	3.96 ± 0.50	0.14
Alanine	1.09 ± 0.09	0.78 ± 0.07	0.03*
Glucose	0.33 ± 0.04	0.79 ± 0.15	0.009*
Glutamine	1.28 ± 0.16	0.97 ± 0.13	0.18
Glutamate	3.10 ± 0.25	2.50 ± 0.16	0.08
Aspartate	0.10 ± 0.02	0.08 ± 0.01	0.39
Glycine	1.06 ± 0.05	1.01 ± 0.14	0.76
Glutathione	1.59 ± 0.32	1.07 ± 0.09	0.19
Creatine	1.30 ± 0.16	1.17 ± 0.53	0.26
Phosphocreatine	0.36 ± 0.10	0.28 ± 0.04	0.50
ATP+ADP	0.98 ± 0.08	0.89 ± 0.08	0.46
Data are expressed as µmol/g wet weight and presented as the mean±sem, n ≥ 5 in each group. Two-tailed unpaired *t* test was used to compare MK2206-treated tumour extracts with vehicle-treated controls and $^{*}P \leq 0.05$ is considered significant.			

Figure 1

A Time/h 6 12 24
MK-2206 − + − + − +

PARP
cPARP
pAKT (Ser473)
AKT
B-Actin
pRPS6 (Ser240/244)
RPS6
B-Actin

B
% Total cell no.
■G1 ■S ■G2
Cont   MK-2206

C
MK-2206
Control

PC
PI
PE GPE GPC PCr NTPγ NTPα NTPβ

PC
GPC PCr/Cr GSH Gln Glu Ac Ala Lac

D
% Control
PC GPC tCho
■6h ■12h □24h

E
% Control
Lac Ala glu gln GSH Cr PCr Gluc
■6h ■12h □24h

Figure 2

A HT29 xenografts

B PC3 xenografts

C